



USING OF VHR SATELLITE IMAGES FOR ROAD NETWORK EXTRACTION IN EGYPT

Beshoy Nady ^{*,1}, Yasser Mostafa ² Yousef A. Abbas, ³, and Mahmoud Enieb ⁴

^{1, 3, 4} *Civil Eng. Dept., Faculty of Engineering, Assiut University, Assiut, Egypt*

² *Civil Eng. Dept., Faculty of Engineering, Sohag University, Sohag, Egypt*

Received 2 September 2019; Accepted 1 October 2019

ABSTRACT

Roads extraction from VHR satellite images are very paramount for GIS and map updating. Due to the high resolution of satellite images, there are many obstacles broken roads such as shadow, and vehicles. The present work aims to find the most suitable road extraction approach that can be applied in the Egyptian environment.

In this study, two satellite images from WorldView-2 and WorldView-3 were used. Classification of image by pixel-based and object-based was carried out to find the appropriate classification method for road extraction. Then, road class refinement by morphology and angular texture signature are performed to decrease the misclassifications between roads and other spectrally similar objects. After that, an iterative and localized Hough transform method was compared with the thinning algorithm method to find the proper method that can extract road centerline segments from the refined images. The performance of the extracted roads was estimated by using the common metrics; completeness, correctness, and quality. The results of this work demonstrate that the random tree in object-based classification achieves the highest overall accuracy than other classification methods. Also, thinning algorithm has more advantages than Hough transform.

Keywords: Road network, Hough transform, thinning algorithm, morphology, road centerline extraction, and classification.

1. Introduction

In the last years, many new cities and a big road network were constructed in Egypt [1]. It is necessary to update the roadmaps and Geographical Information System (GIS) database. Road extraction is a great significance for vehicle navigation, traffic management, road monitoring, urban planning, and map updating, etc. [2]. Manual road network extraction can be used for aerial or satellite images if the concerned area is small, but it is not possible when the area is big. The automatic road extraction is merit studying and sometimes extremely needed. Automatic road extraction from satellite images is challenging problem, because of

* Corresponding author.

E- mail address: beshoynady112@gmail.com

the diversity of road pavement materials (the road surface partially repaired) and occlusion (e.g. shadows of trees and buildings, vehicles and traffic markings, etc).

Many researchers presented different strategies for road extraction [3]. The first set of studies concentrates on road recognition by using their geometric properties, such as radon transform [4] and mathematical morphology [5], [6]. The second set of methods concentrates on the variance between roads and their neighbor such as active contour models also called snakes [7]. The third set of studies for road extraction depends on image classification by using the spectral properties of road materials from multispectral satellite images. The pixel-based classification is the most classical methods based on the spectral information only like the maximum likelihood classifier. Also, object-based classification is a popular classification method, where the element consists of a set of pixels (segments) rather than a single pixel. This method makes use of important characteristics (shape, texture, and contextual characteristics) that is solely in meaningful image objects and their common relationships [8]. The present work aims mainly to find the most suitable road network extraction approach that can be applied in the Egyptian environment.

The rest of this work is organized as follows. Road network extraction is reported in section 2. Results and discussion illustrated in section 3. Lastly, conclusions are discussed in section 4.

2. Road network extraction

In this research, roads extraction from remote sensing images passes through the following steps: data fusion, classification, assessment of classification, classification refinement, centerline extraction, road network formation and assessment of road network extraction (Fig. 1).

2.1. Data fusion

To take advantage of spatial/spectral resolution characteristics of satellite images for feature extraction, data fusion techniques are needed [9]. Two study areas from very high-resolution satellite images are used. The study area is located at Assiut governorate, Egypt. Assiut is one of the fastest-growing urban areas in Egypt [10]. The main land cover of the area is consists of road networks, residential area, vegetation, and bare soil.

The first study area was selected from WorldView-3 satellite image (Pan + 8 MS bands) captured in September 13, 2016 for New Assiut city cover $1202 \times 1248 \text{ m}^2$. The second study area was selected from WorldView-2 satellite (Pan + 8 MS bands) captured in March 4, 2016 from Assiut city (Golta Company) cover $539 \times 444 \text{ m}^2$. WorldView- 2 satellite is the first high-resolution 8-band multispectral commercial satellite, launched October 8, 2009. Where, WorldView- 3 satellite was successfully launched on August 13, 2014. WorldView- 2 and WorldView- 3 can collect data with 0.5 m resolution for panchromatic image and 2.0 m for the multispectral image.

The pansharpening process was performed in the two used images using Principal Component Analysis (PCA) technique by ERDAS IMAGINE 2013 software. Resampling by the nearest neighbor method was selected to make the color content of the original multispectral image unchanged (Fig. 2).

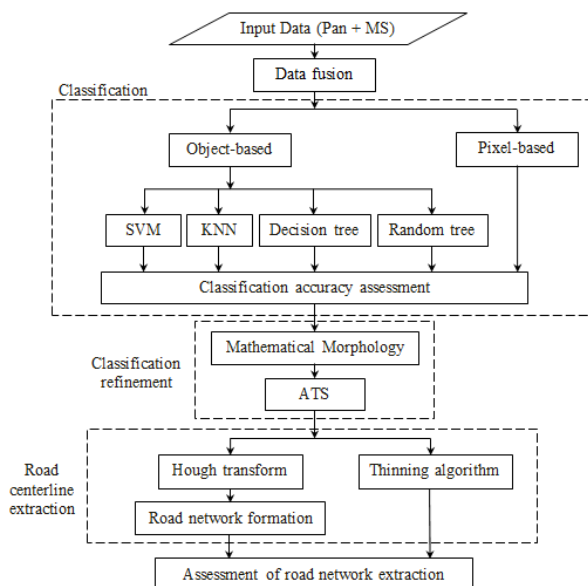


Fig. 1. Flowchart of the proposed procedure.



Fig. 2. The study area-Assiut governorate, Egypt: (a) WorldView- 3 satellite image for New Assiut city, and (b) WorldView- 2 satellite image for Assiut city.

2.2. Image classification

2.2.1. Pixel-based classification

Pixel-based method depends only on the pixel spectral information to extract features without taking into consideration the spatial relationship between the neighboring pixels. There are two main methods for pixel-based classification: unsupervised and supervised classification.

2.2.2. Unsupervised classification

Unsupervised classification is more convenient in an automatic classification process, where the training samples were not needed to enter, in practice, the evaluation of results depend on the user's expectations. Unsupervised classification creates a useful indication of detectable classes for supervised classification. By applying unsupervised classification in ERDAS IMAGINE 2013 for study areas, five classes were recognized. These classes are roads, building, vegetation, shadow, and bare soil.

2.2.3. Supervised classification

The supervised classification depends on selecting the training samples which give information for each class. Then the classification process was performed using

classification algorithm. There are many pixel-based classification algorithms such as minimum-distance, Mahalanobis and maximum likelihood. Maximum likelihood is used in this research, as it takes the variability of classes into account and gives better results [11].

Pixel-based image classification by maximum likelihood method is implemented after selecting training samples. In the first study area, the resulted thematic image contains building, road, shadow, vegetation, and bare soil classes. In the second study area, the resulted thematic image contains building, road, shadow, vegetation, and railway. The shadow class reclassified to the road class (Fig. 3 - b). The thematic images resulted from classification are converted into a binary image, where road class is white (pixel value = 1) and other classes are black (pixel value = 0).

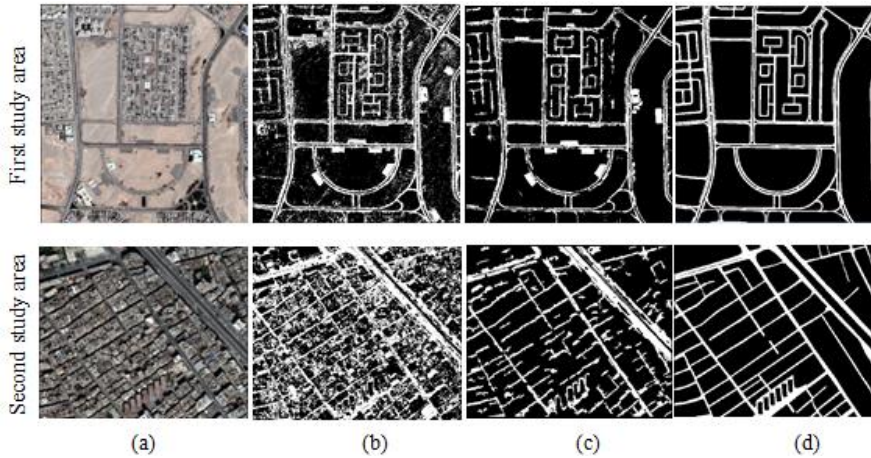


Fig. 3. Classification results of two images: (a) input image, (b) results of pixel-based classification, (c) results of object-based classification, and (d) ground truth.

2.2.4. Object-based classification

In object-based classification, the groups of pixels which similar in spectral properties are merged to make an object. The basic principle of object-based is using the paramount information (texture, contextual and shape information). Object-based image analysis includes two stages, image segmentation, and image classification.

2.2.4.1. Image segmentation

Image segmentation divides an image into separated regions according to some specified parameters. Scale, shape, and compactness are the three parameters used to affect the multiresolution segmentation result. Where scale parameter controls the average size of objects. Shape, and compactness parameters control the homogeneity of objects. In this research, a multiresolution segmentation technique; was performed in eCognition software. The appropriate values of parameters are selected depend on the trial and error method. The selected parameters are; scale 30, shape 0.2 and compactness 0.5 for the first study area, and scale factor 50, shape 0.5 and compactness 0.5 for the second study area.

2.2.4.2 Object classification

In object classification stage, training samples are selected for each land cover class. Then classification algorithms; k- nearest neighbor, support vector machine, decision tree, and random tree were applied. For road classification the following object attributes were considered: Normalized Difference Vegetation Index (NDVI) in detecting vegetation (Eq.1), Built-up Area Index (BAI) (Eq.2) in enhancing asphalt and concrete surfaces

information [12]. Also, length/width ratio value, standard deviations, relative border to, spectral mean and area of objects are used.

$$\text{NDVI} = \frac{\text{NIR} - \text{Red}}{\text{NIR} + \text{Red}} \quad (1)$$

$$\text{BAI} = \frac{\text{Blue} - \text{NIR}}{\text{Blue} + \text{NIR}} \quad (2)$$

Where *NIR*, *Red*, *Blue* are the Near-Infrared, Red, and Blue bands respectively.

In KNN *K* was taken equal 1, SVM (kernel type rbf, *C*=2, and *gamma*=5), whilst decision tree and random tree were selected as default in the first study area in eCognition Developer 9.0. In the second study area, *K* in KNN taken equal 3, SVM (kernel type rbf, *C*=5, and *gamma*=5) decision tree and random tree were selected as default (these parameters were selected by trials).

The process tree is implemented by using mean *NIR*, *NDVI*, *BAI*, Asymmetry, length/width, standard deviation, relative border to, rectangular fit, width, area, and merge region for objects. The thresholds of these parameters are manually selected. The roads have a high value of length/width and there width is constant, so these features are used to distinguish between the roads and buildings. The vegetation areas are extracted by using *NDVI* and mean *NIR*, and the *BAI* is used to extract bare soil. The buildings objects have standard deviation higher than both roads and bare soil due to non-homogeneity in the building. The yellow band is used to extract sand class in the first study area (desert area). The results are transformed to binary image. Fig. 3 – c shows the results of the random tree method for first and second study areas.

2.3. Classification accuracy assessment

The binary image is a result of classification where road pixels are white and non-roads are black. The assessment of the results is performed by using the four metrics defined in [13]. The data of ground truth obtained via manual digitization. To evaluate the results, the extracted road network is compared with ground truth and four values are computed as follows.

$$\text{Completeness} = \frac{TP}{TP + FN} \quad (3)$$

$$\text{Correctness} = \frac{TP}{TP + FP} \quad (4)$$

$$\text{Quality} = \frac{TP}{TP + FP + FN} \quad (5)$$

$$\text{Accuracy} = \frac{TP + TN}{TP + TN + FP + FN} \quad (6)$$

In which, True Positive (*TP*) is the number of road pixels detected correctly, False Negative (*FN*) is the number of road pixels detected as non-road, False Positive (*FP*) is the number of non-road pixels detected as roads, True Negative (*TN*) is the number of non-road pixels detected correctly. Completeness, correctness, quality, and overall accuracy are calculated for the study areas (table 1).

2.4. Classification refinement

The main problem is the spectral similarity between the roads and parking lots or buildings. So refinement of classification results is demanded to remove the non-road regions, fill gaps, and trim road regions before extraction of the road centerline and

formation road network. Refinement of the road region is obtained by using two stages; mathematical morphology and Angular Texture Signature (ATS).

2.4.1. Mathematical morphology

Mathematical morphology is considered as a filter through pre- or post-processing operations. The two primary mathematical morphology operations are erosion and dilation that can be used to obtain more complex operations. The opening operation could be used to separate small region from larger road region whilst preserving the shape of the road region. Closing could be used to fill small gaps and connect road region, whilst also preserving the shape of the objects [14].

In this study, the closing mathematical morphology is used to fill the small holes and to trim the road class in the binary image resulted from classification. The size 5×5 of closing morphology is implemented in ERDAS IMAGINE 2013.

2.4.2. Angular texture signature

The binary image resulted from applying morphology, still contain non-road regions (parking lots and buildings) classified as road region. Zhang and Couloigner [15] modified the Angular Texture Signature (ATS) and performed this method in a binary image instead of a grayscale image and for road pixels only. ATS method is calculated by the sum of road pixels within the rectangular region divided by the total pixels to get the mean value. The rectangular region is calculated every 20 degree for each pixel. The rectangular width is taken as road width in the study area, and the length is twice its width. By drawing the mean values in each direction around the pixel and connected these points, closed polygon called ATS polygon has resulted. Four shape descriptors (mean, compactness, eccentricity, and direction) are calculated from ATS polygon to separate between road and parking lots/buildings regions.

In this study, ATS is implemented by writing a code program in MATLAB R2015b. The size of the rectangular window is taken 19 by 38 pixels. The result of ATS after applying closing morphology method for the first study area is showed in Fig. 4, and closing morphology in the second study area is showed in Fig. 5.

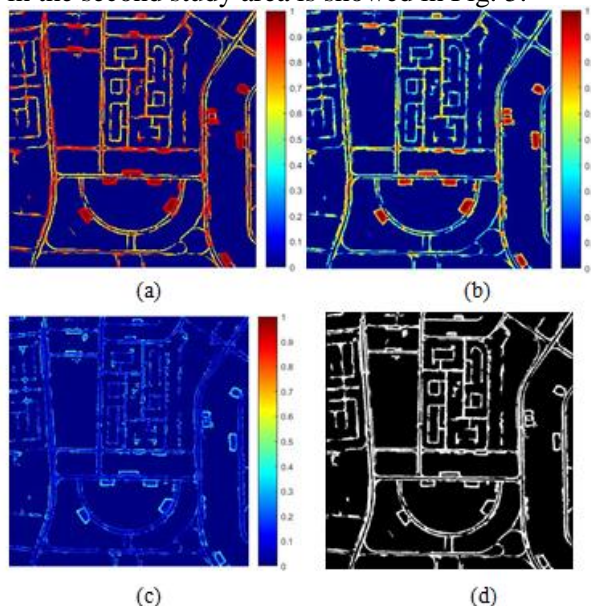


Fig. 4. Results of classification refinement for the first study area: (a) ATS compactness, (b) mean, (c) eccentricity, and (d) result of morphology and ATS refinement.



Fig. 5. Result of classification refinement by closing morphology for the second study area.

2.5. Road centerline extraction

The road centerline extraction from remote sensing images has several implementations, such as road map and GIS updating, etc. There are shortcomings in centerline extraction of the road due to occlusions and noise. In this study, the thinning algorithm and Hough transform are used to extract road centerline.

2.5.1. Thinning algorithm

The thinning process was performed in a binary image in a two-pass erosion process that is defined as a process of removing one pixel from the border of one object. Firstly, pixels achieving the condition of normal erosion were defined as candidates for removing. Secondly, the candidates pixels that not break the connectivity of the object were removed. All road segments by the thinning process became one pixel wide. The result of the thinning process is raster image, so vectorization procedure is applied to convert raster images to vector images.

The thinning algorithm is implemented in binary images that refined in the previous step to extract road centerline. The thinning process reducing processing time and effective in curvilinear roads, but the main problem is spurs as shown in fig. 6 – a. The results of extracted road centerline were compared with reference maps for the two study areas. The reference map for the first study area was produced in 2015 with 1:1000 scale, and for the second study area in 2002 with 1: 5000 as shown in fig. 6 – b.

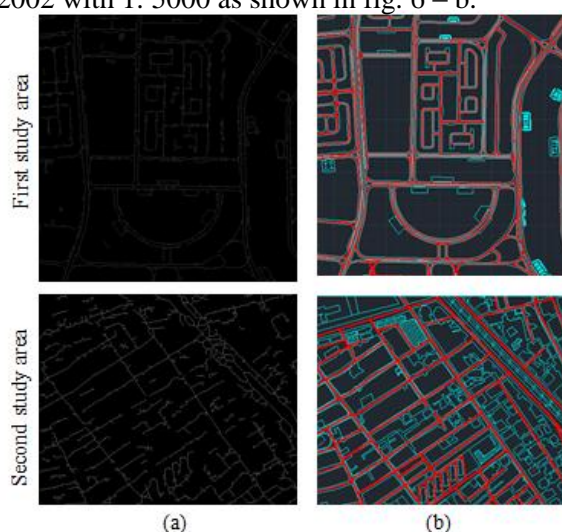


Fig. 6. Extracted road centerlines by thinning algorithm (a) Thinning algorithm results, and (b) maps of road centerlines for the two study area.

2.5.2. Hough transform and road network formation

In Hough Transform (HT) each line in the image space, defined by the slope parameter and the y-intercept parameter, is transformed to a point in the parameter space. In the parameter space, each point has amplitude according to the points located on the line in image space. The purpose of the Hough transform is finding the peak in the parameter space (fig. 7 - a). One of the merits of the HT is relatively uninfluenced by fragmentation and random noise [16].

Zhang and Couloigner [4] developed an iterative radon transform and applied on binary image to extract road centerlines. Also, the localization of the radon transform was applied to make peaks appear clearly to extract small road segments and long curvilinear roads. In this study, iterative and gliding box approach for localized Hough transform is used. The size of the used gliding box for localized Hough transform is 200 by 200 pixels for the first study area and 400 by 400 pixels for the second study area. After applying HT, the disconnected road segments are needed to be linked for getting meaningful road lines and setting up the road network formation to make the data suitable for GIS.

In this research, the results are intersected short lines due to using the iterative Hough transform and also curvilinear roads. Intersection inner point between each two lines is detected, and then a fitting curve passes through these points is drawn (blue lines in fig. 7 - c and fig. 8 - b). The Euclidean distance between endpoints in each two lines is checked. If Euclidean distance is less than a threshold equal to 15 pixels, the new merged point is calculated as the mean of these two endpoints. The last step is checking the length of lines and deletes the lines shorter than the threshold as shown in fig. 7 - c and fig. 8 - b.

The results of the Hough transform showed in fig. 7 - c and fig. 8 - a. In the extracted road centerlines, the single road has a lot of parallel extracted lines due to the using of iterative Hough transform.

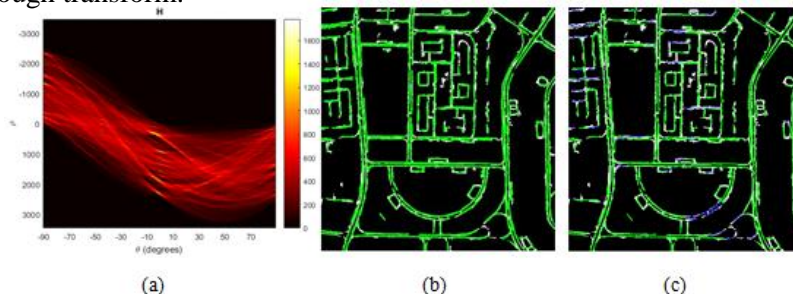


Fig. 7. Road centerlines extraction by Hough transform for the first study area (a) the Hough transform for the entire refined image in (fig. 4 – d), (b) extracted road centerlines, and (c) results of network formation.

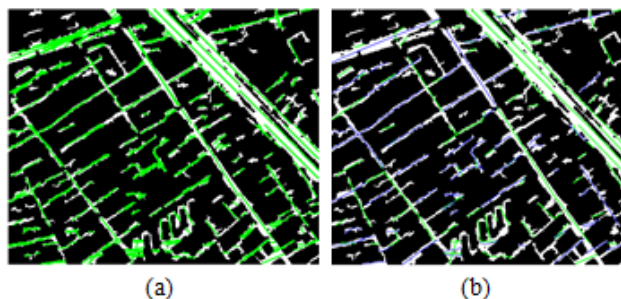


Fig. 8. Road centerlines extraction by Hough transform for the second study area (a) the extracted road centerlines, and (b) results of network formation.

2.6. Assessment of road network extraction

To validate the road network, the comparability between the extracted roads and the reference road maps is performed. The performance of the road extraction is adopted by using three common metrics, completeness, correctness, and quality. A buffer with constant width is built around the extracted road. The part of reference road which is located in the buffer zone is called “matched reference” and the other part is called “unmatched reference”. Around the reference road the same width buffer is built. The portion of the road centerline in the buffer zone is called “matched extraction” (Fig. 9). The lengths of matched reference, unmatched reference, matched extraction, reference road centerline, and extracted road centerline network are calculated. The accuracy of the road extraction is evaluated using; completeness, correctness, and quality. The results of road centerline extraction were compared with the reference maps for the two study areas as shown in table 2.

$$\text{Completeness} = \frac{\text{length of matched reference}}{\text{length of reference}} \quad (7)$$

$$\text{Correctness} = \frac{\text{length of matched extraction}}{\text{length of extraction}} \quad (8)$$

$$\text{Quality} = \frac{\text{length of matched extraction}}{\text{length of extraction} + \text{length of unmatched reference}} \quad (9)$$

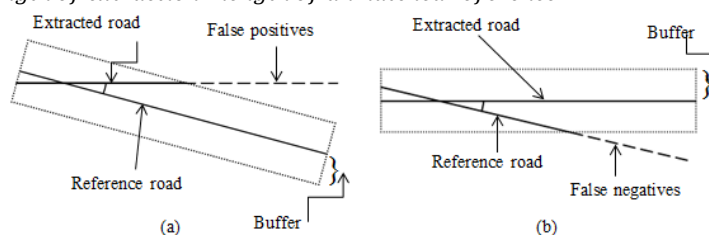


Fig. 9. Assessment of road network extraction: (a) comparison of the extracted image, and (b) comparison of the reference image.

3. Results and discussion

Fig. 3 - b shows the results of pixel-based classification. The first study area, through the visual examination, shows acceptable results since the study area is good planned and there roads are wide. To evaluate the results, the comparability between the binary image and the manual digitization ground truth (Fig. 3 – d) is implemented. In the second study area, the result is not satisfied because the study area is semi-planned and the roads are narrow. Completeness, correctness, quality, and overall accuracy are calculated for the study areas (table 1). The results show that the completeness is high 73.60%, but correctness 35.15% is very low due to considering shadow as a road. The quality value 31.22% and overall accuracy 66.67% are very low.

The object-based classification results were showed in table 1 for the two study areas. The results of the first study area are high due to the good planning for the new Assiut city and the road width. In the second study area, results are low because of their narrow roads and the buildings have different heights so part of the shadow that considered roads are buildings. The main reason for misclassified in the first study area is due to the presence of sand that covers the road partially or totally. Parking lots and road have the same material (Asphalt) so the classification method cannot distinguish between them. The main reasons for the misclassification in the second study area are the traffic jam, parking beside roads and the railway classified as a road.

The results of object-based classification methods are nearby but in the first study area, the random tree method has high completeness, correctness, quality, and overall accuracy (71.76%, 82.89%, 62.50%, and 91.49% respectively). In the second study area, the random tree method has high completeness, quality, correctness and overall accuracy (67.78%, 60.88%, 47.22, and 84.51% respectively). The resulted images of the random tree method were used for the next step.

Table 1.

The results of classification for study areas by pixel-based and object-based.

		Pixel-based	Object-based classification			
		Maximum likelihood	KNN	SVM	Decision tree	Random tree
First study area	Completeness%	78.65	65.84	63.87	67.98	71.76
	Correctness%	54.89	82.21	82.31	82.03	82.89
	Quality%	47.77	57.63	56.16	59.17	62.50
	Overall accuracy%	83.57	90.75	90.47	91.03	91.49
Second study area	Completeness%	73.60	66.39	66.85	64.73	67.78
	Correctness%	35.15	58.01	59.19	59.25	60.88
	Quality%	31.22	44.84	45.76	44.79	47.22
	Overall accuracy%	66.67	83.65	84.13	84.02	84.51

Fig. 4 and Fig. 5 show the mathematical morphology and ATS results for the first and second study areas respectively. The results show obviously the influence of mathematical morphology and ATS on refining the road class from parking lots and buildings.

To assess the results of network formation of the Hough transform and thinning algorithm, the results of extracted road centerline were compared with reference maps for the two study areas. The lengths of reference and extracted centerlines are estimated. The completeness, correctness, and quality are calculated as shown in table (2). The results show that the thinning algorithm has high values of both completeness and quality. Hough transform has a high value of correctness than the thinning algorithm due to the spurs in thinning algorithm results. Also, the thinning algorithm is appropriate for curvilinear roads than the Hough transform. So the thinning algorithm is better than the Hough transform.

Table 2.

The results of extracted road centerlines for first and second study areas.

	First study area		Second study area	
	Hough transform	Thinning algorithm	Hough transform	Thinning algorithm
Completeness%	84.51	89.97	70.09	80.64
Correctness%	93.11	91.27	79.21	71.12
Quality%	78.82	82.57	56.66	61.11

4. Conclusions

This paper aims to find the most suitable road network extraction approach that can be applied in the Egyptian environment.

- The random tree in the object-based gave the higher accuracy than SVM, KNN, decision tree, and pixel-based. The random trees' completeness, correctness, quality,

and overall accuracy were 71.76, 82.89, 62.50, and 91.49 for the first study area and the second study area were 67.78, 60.88, 47.22, and 84.51 respectively.

- Closing morphology improved and refined the results of classification significantly. The separation of parking lots and buildings from road class achieved obviously by using ATS.
- The centerline of roads extracted by the thinning algorithm is higher accuracy than the Hough transform.
- The proposed approach is effective to update maps and GIS database in the Egyptian environment.

REFERENCES

- [1] Hashim, I. H., Abdel-Wahed, T. A., and Moustafa, Y., 2016. "Toward an operating speed profile model for rural two-lane roads in Egypt." *J. Traffic Transp. Eng.*, Vol. 3, No. 1, pp. 82-88.
- [2] Shi, W., Miao, Z., Wang, Q., and Zhang, H., 2014. "Spectral-spatial classification and shape features for urban road centerline extraction". *IEEE Geosci. Remote Sens. Lett.* 11, 788–792.
- [3] Miao, Z., Shi, W., Gamba, P., and Li, Z., 2015. "An Object-Based Method for Road Network Extraction in VHR Satellite Images". *IEEE Journal of Selected Topics in Applied Earth Observations and Remote Sensing*, Vol. 8, No. 10, pp. 4853-4862.
- [4] Zhang, Q., and Couloigner, I., 2007. "Accurate centerline detection and line width estimation of thick lines using the radon transform". *IEEE Trans. Image Process*, Vol. 16, No. 2, pp. 310-316.
- [5] Sujatha, C., and Selvathi, D., 2015. "Connected component-based technique for automatic extraction of road centerline in high resolution satellite images". *EURASIP J. Image Video Process.*, Vol. 1, pp. 8.
- [6] Reshma, S. B., Radhakrishnan, B., and Suresh, L. P., 2016. "Detection and extraction of roads from satellite images based on Laplacian of Gaussian operator". In *International conference on emerging technological trends (ICETT)*.
- [7] Nakaguro, Y., Makhanov, S. S., and Dailey, M. N., 2011. "Numerical experiments with cooperating multiple quadratic snakes for road extraction". *Int. J. Geog. Inf. Sci.*, Vol. 25, No. 5, pp. 765–783.
- [8] Chen, L., Zhu, Q., Xie, X., Hu, H., and Zeng, H., 2018. "Road Extraction from VHR Remote-Sensing Imagery via Object Segmentation Constrained by Gabor Features". *ISPRS Int. J. Geo-Inf.*, Vol. 7, No. 9, pp. 362.
- [9] Mostafa, F., Mostafa, Y., and Yousef, M., 2014a. "The optimal method for classifying high resolution satellite images in Egypt environment". *Journal of Engineering Sciences Assiut University*, Vol. 42, No. 4, pp. 1106-1121.
- [10] Farrag, A., and Mostafa, Y., 2006 "Comparison of Land Cover Change Detection Techniques with Satellite Images: Case Study in Assiut, Egypt" *Civil Engineering Research Magazine, Al-Azhar University*, Vol. 28, No. 3, pp. 983-996.
- [11] Mostafa, F., Mostafa, Y., Yousef, M., and Abas, A., 2014b. "Using of High Resolution Satellite Images for Updating Large Scale Mapping in EGYPT" *Journal of Engineering Sciences, Assiut University, Faculty of Engineering*, Vol. 42, No. 4, pp. 1122-1137.
- [12] Mhangara, P., Odindi, J., Kleyn, L., and Remas, H., 2011. "Road extraction using object oriented classification". *Visualisation Technical*, pp.45-50.
- [13] Sun, K., Zhang, J., and Zhang, Y., 2019. "Roads and intersections extraction from high-resolution remote sensing imagery based on tensor voting under big data environment". *Wireless Communications and Mobile Computing*, Vol. (2019).
- [14] Gonzalez, R. C., and Woods, R. E., 2008. "Digital image processing (Third Edition)". Prentice-Hall, Inc., Upper Saddle River.
- [15] Zhang, Q., and Couloigner, I., 2006. "Benefit of the angular texture signature for the separation of parking lots and roads on high resolution multispectral imagery", *Pattern Recognit. Lett.*, Vol. 27, No. 9, pp. 937-946.
- [16] Liu, W., Zhang, Z., Li, S., and Tao, D., 2017. "Road detection by using a generalized Hough transform", *Remote Sens.*, Vol. 9, No. 6, pp. 590.

استخدام مرئيات الاقمار الصناعية عالية الدقة لاستخراج شبكات الطرق في مصر

الملخص العربي

يعد استخراج شبكات الطرق من صور الاقمار الصناعية عالية الجودة بغرض تحديث نظم المعلومات الجغرافية والخرائط تحديا كبيرا في موضوعات البحث العلمي. حيث تظهر العديد من العقبات والعوائق التي تغطي الطرق كليا او جزئيا مثل السيارات وظل الاشجار والمباني. يهدف هذا البحث لإيجاد انسب طريقه لاستخراج شبكات الطرق يمكن تطبيقها في البيئة المصرية.

أجريت الدراسة باستخدام مرئيتين من مرئيات الاقمار الصناعية (WorldView-3, WorldView-2) لمدينة أسيوط الجديدة ومدينة أسيوط. حيث تم المقارنة بين طريقتي التصنيف (pixel-based classification)، (object-based classification) لاستخراج شبكات الطرق. ولتحسين تصنيف الطرق وتنقيتها من الأشياء المماثلة لها في الطيف استخدمت طريقتي (Morphology, Angular Texture Signature (ATS)). بعد ذلك تم استخدام طريقة Hough التكرارية وتطبيقها علي الصورة بعد تقسيم الصورة الي اجزاء (Iterative and localized Hough transform) و تكوين شبكة الطرق (من اجزاء الطرق التي تنتمي لنفس الطريق) ومقارنتها بطريقة التخفيف (thinning algorithm) لإيجاد الطريقة الملائمة لاستخراج محور الطريق. استخدم برنامج ايرداس ايماجن 2013 للتصنيف بطريقة البكسل وبرنامج ايكوجناش 9 في التصنيف بطريقة الكائنات. استخدم الماتلاب في كتابة كود لكل من (ATS, thinning algorithm, Hough transform and network formation). أظهرت النتائج أن التصنيف بطريقة random tree المطبقة في object-based classification وكذلك طريقة التخفيف thinning algorithm المستخدمة في استخراج محور الطرق، هما الانسب لهذه الدراسة.